Applied Physics Letters

Influence of dislocations on thermal conductivity of strontium titanate

Cite as: Appl. Phys. Lett. **117**, 021902 (2020); https://doi.org/10.1063/5.0010234
Submitted: 08 April 2020 • Accepted: 24 June 2020 • Published Online: 13 July 2020

Melanie Johanning, Lukas Porz, Jinfeng Dong, et al.

AIP Publishing

Applied Physics Letters ARTICLE scitation.org/journal/apl

Influence of dislocations on thermal conductivity of strontium titanate

Cite as: Appl. Phys. Lett. **117**, 021902 (2020); doi: 10.1063/5.0010234
Submitted: 8 April 2020 · Accepted: 24 June 2020 ·
Published Online: 13 July 2020

Melanie Johanning,[1,a)] Lukas Porz,[1,a)] Jinfeng Dong,[2] Atsutomo Nakamura,[3,4] Jing-Feng Li,[2] and Jürgen Rödel[1]

AFFILIATIONS

[1]Division of Nonmetallic-Inorganic Materials, Department of Materials and Earth Sciences, Technical University of Darmstadt, 64287 Darmstadt, Germany
[2]State Key Laboratory of New Ceramics and Fine Processing, Department of Materials Science and Engineering, Tsinghua University Beijing, Beijing 100084, People's Republic of China
[3]Department of Materials Physics, Nagoya University, Furo-cho, Chikusa-ku, Nagoya 464-8603, Japan
[4]PRESTO, Japan Science and Technology Agency (JST), 7, Gobancho, Chiyoda-ku, Tokyo 102-0076, Japan

[a)]**Authors to whom correspondence should be addressed:** melanievictoria.johanning@stud.tu-darmstadt.de and porz@ceramics.tu-darmstadt.de

ABSTRACT

Recently, several creative processing techniques yielded thermoelectrics with reduced thermal conductivity and, thereby, an enhanced figure or merit. These were based on engineered complex microstructures with attendant dislocation structures. In this study, we implement highly controlled mesoscopic dislocation structures into the model thermoelectric $SrTiO_3$ in order to quantify phonon scattering at dislocations. Both single crystals and polycrystalline material have been furnished with enhanced dislocation densities increased by a factor of 150–300 by plastic deformation. Thermal conductivity was measured using laser flash analysis between room temperature and 325 °C. Etch pit techniques and ultra-high voltage electron microscopy afford quantification of dislocation density. Experimental results were compared to predictions by the Debye-Callaway model. The latter revealed that dislocation densities of 10^{15} m^{-2} would be necessary for the reduction of thermal conductivity of $SrTiO_3$ in the investigated temperature range, which could not be realized using the plastic deformation mechanism applied.

Tuning of thermal properties is considered a key avenue to train thermoelectrics for the marketplace.[1,2] To this end, point defects have been considered extensively in the past.[3] Dislocations are similarly suggested to have great potential in tailoring the thermal conductivity.[1,2] In particular, several creative processing techniques have been developed recently, like liquid phase compaction[4] or melt centrifugation.[5] These materials reveal a very complex microstructure. For melt-centrifuged $(Bi,Sb)_2Te_3$, dislocation networks at the grain boundary with a dislocation density of 2×10^{14} m^{-2}, estimated from the mean dislocation distance of 5 nm in the grain boundary,[5] are produced. This average volume density does, however, not reflect the highly non-uniform distribution of dislocations. While the new microstructures appear to be promising to enhance the figure of merit of thermoelectrics by dislocations,[2,6,7] their convoluted microstructure does not allow us to extract the impact of dislocations on properties unequivocally.

The influence of dislocations on phonon transport has been studied in theory since the 1950s.[8,9] The strain field and dislocation core[8] are suggested to reduce the phonon mean free path (MFP) and, thus, reduce thermal conductivity, depending on phonon frequency and dislocation density.[8] Experimental evidence of phonon scattering by dislocations was attained in plastically deformed single crystals at cryogenic temperatures,[10] where the intrinsic MFP is large and can, thus, be reduced with lower dislocation densities compared to room temperature. A recent study suggests that above a critical dislocation density, dislocations can reduce thermal conductivity even at room temperature,[11] where intrinsic scattering gets more dominant.

In this study, we fundamentally address the impact of the mesoscopic dislocation structure with a well-defined density on thermal conductivity. Evaluation is facilitated using single crystal reference material and is contrasted with/compared to polycrystalline specimen. As an experimental tool, we apply plastic deformation as a means with

high control to introduce dislocations. Many ceramics, among them potential thermoelectrics, can be deformed plastically at room temperature or elevated temperatures.

Strontium titanate ($SrTiO_3$) serves as well-studied model material. The defect chemistry,[12] plastic behavior,[13,14] slip systems,[15] and thermal properties[16,17] are well known. Furthermore, functional properties of $SrTiO_3$ are important for its applications, e.g., as a potential thermoelectric,[18,19] particularly at high temperatures.[20] However, high thermal conductivity still limits its competitiveness.[19]

We were able to produce well-oriented dislocation structures of ⟨100⟩{100} dislocations in [110]-oriented $SrTiO_3$ single crystals by deformation at 1050 °C. Beyond that, we were able to plastically deform polycrystals to introduce dislocations. Laser flash analysis (LFA) between room temperature and 325 °C was utilized to probe the thermal conductivity of plastically deformed samples and undeformed reference samples. Dislocation densities were quantified using etch pit techniques as well as ultra-high voltage electron microscopy.

Ordered dislocation structures were introduced by plastic deformation under uniaxial compression (Z010, Zwick GmbH & Co. KG, Ulm, Germany). Reference samples of identical crystal orientation, temperature profile, polishing procedure, and sample thickness were utilized to quantify the impact of dislocations on thermal conductivity. Undoped $SrTiO_3$ single crystals with a nominal purity of 99.99% and a size of 4 mm × 4 mm × 8 mm, commercially available from Alineason Materials Technology GmbH (Frankfurt am Main, Germany), were probed.

Deformation of a [110]-oriented single crystal at 1050 °C results in a network of ⟨100⟩{100} dislocations. The experimental steps are illustrated in Figs. 1(a)–1(c). A notch with a depth of ∼1 mm was cut into the (1-10)-surface using a wire saw with a wire diameter of 170 μm. This results in a stress concentration that enhances the dislocation density. A suitable choice of crystal orientation and temperature allows us to only activate one slip system with the highest Schmid factor at a time.[14] A total displacement of 17 μm was attained for the 8 mm high crystal.

In order to quantify the local dislocation density, sample surfaces were etched with a solution of 16 drops of 50% HF (H_2O) in 15 ml of 50% HNO_3 (H_2O). While distributed in the whole sample, dislocations arrange preferably in glide planes at an angle of 45° to the notch. Therefore, slices at an angle of 45° were extracted and thermal conductivity was determined perpendicular to the sample surface in order to maximize the potential scattering influence. Slices were shaped by careful grinding in order to avoid damage during cutting. The samples were prepared by standard polishing (Phoenix 4000, Buehler, ITW Test & Measurement GmbH, Esslingen am Neckar, Germany) followed by vibrational polishing (Jean Wirtz DBP Nr. 1 118 045). Etch pit density on the surface after HF-etching was taken as proof that polishing damage could be avoided. The final sample thickness of both deformed and reference samples was 1030 μm. Dislocation density was examined using an ultra-high voltage electron microscope (UHVEM; JEOL JEM-1000k RS) operated at 1000 kV for samples from the same type of crystals deformed by 2% without a notch.

Thermal conductivity was determined between room temperature and 325 °C by the calculation from thermal diffusivity measured by laser flash analysis or LFA (LFA 457, Erich NETZSCH GmbH & Co. Holding KG, Selb, Germany). Samples were sputtered with a reflective Pt-coating to prevent direct transmission of the laser. A

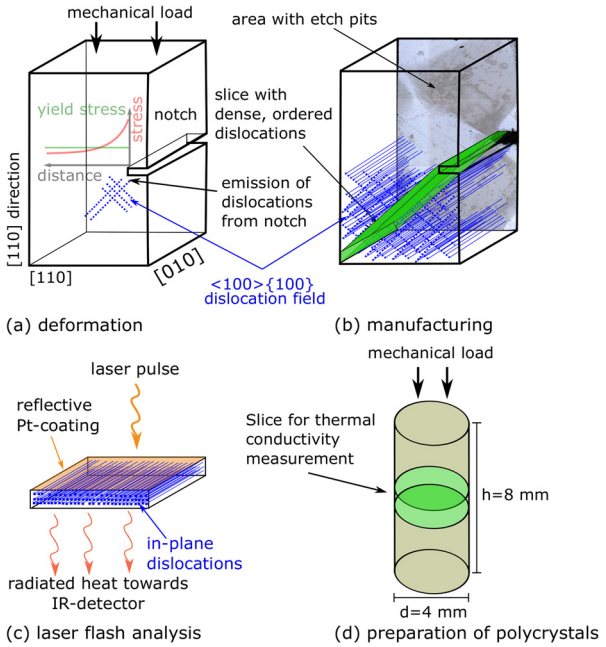

FIG. 1. Processing steps for samples with an ordered ⟨100⟩{100} mesoscopic structure of dislocations (a)–(c). Deformation of single crystals leads to emission of dislocations from the notch, and dislocation fields are formed (a). Etched samples reveal the dislocation network shown in the background. Slices were extracted at an angle of 45° to the notch (b). LFA measurements were performed perpendicular to the glide planes (c). Polycrystalline cylinders were deformed, and slices were cut from the cylinder for LFA measurements (d).

density of 5.03 g cm^{-3}, obtained by the Archimedes method, heat capacity, assumed as the Dulong–Petit limit of 3 R, equivalent to 670 J kg^{-1} K^{-1} for $SrTiO_3$, and the sample thickness were taken as constant. Additional quantification of samples with ⟨110⟩{110} dislocation bands, experimentation with Fe- and Nb-doped samples, and model calculations were conducted for verification of the results (see the supplementary material).

Undoped $SrTiO_3$ polycrystals were produced by sintering for 1 h at 1425 °C in a pure oxygen atmosphere. After cooling down to room temperature, samples were reheated and held at 1350 °C for 15 h in a pure oxygen atmosphere before final cooling to room temperature. The diameter of the sintered sample was reduced from 6 mm to 4 mm with a turning lathe before deformation by 1.7% at 1150 °C. A constant load was maintained during cooling to avoid recovery of dislocations. Samples were cut into slices perpendicular to the deformation axis [see Fig. 1(d)]. After final polishing, deviations in the sample thickness could be limited to about 20 μm. The grain size was determined using SEM images of undeformed reference samples. Thermal conductivity and dislocation density were investigated in the same manner as that for the single crystalline samples.

Bright-field scanning transmission electron microscopy (BF-STEM) from UHVEM [see Fig. 2(a)] captures the ⟨100⟩{100} dislocation structure. Enabling the visualization of a highly resolved large area, ultra-high voltage electron microscopy is superior to conventional TEM for this purpose. Laser microscope images of etched sample surfaces [Fig. 1(b), for details, see supplementary material (Fig. S1)]

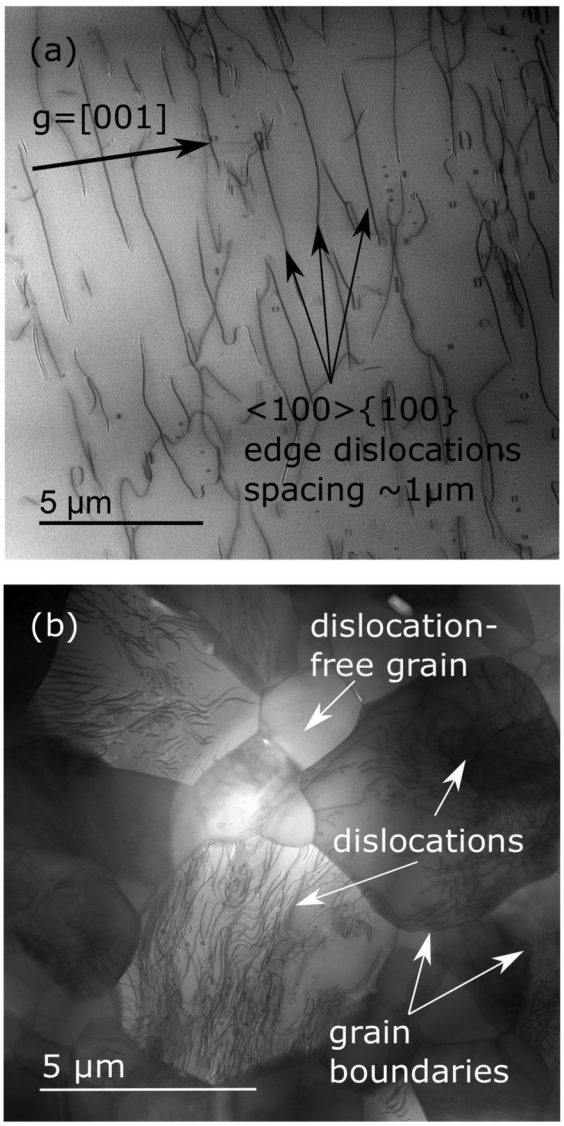

FIG. 2. Image from ultra-high voltage electron microscopy of a single crystal, deformed at 1050 °C by ~2% (a), and a polycrystal, deformed at 1150 °C by 1.7% (b), visualizing the mesoscopic dislocation network.

also attest the successful introduction of well-ordered ⟨100⟩{100} dislocations. The dislocation density increased from the natural dislocation density of $7 \times 10^9\,\mathrm{m}^{-2}$ to $10^{12}\ \mathrm{m}^{-2}$ after deformation. Hence, the mean distance of dislocations is ~1 μm after deformation. As samples for electron microscopy were cut from crystals deformed without a notch, the attained values represent a lower limit of dislocation density for the samples measured with LFA.

The microstructure of polycrystalline samples is visualized by UHVEM [see Fig. 2(b)]. The average grain size of the polycrystal was quantified to be $2.6 \pm 1.5\ \mu$m from SEM images. While the dislocation density after deformation strongly varies between the grains, it is estimated to be $2 \times 10^{12}\ \mathrm{m}^{-2}$ on average. This is to be compared with a dislocation density of $6 \times 10^9\ \mathrm{m}^{-2}$ in the undeformed material.

Measurements of thermal conductivity (see Fig. 3) reveal that there is no significant influence of plastic deformation on thermal conductivity of $SrTiO_3$ between room temperature and 325 °C. Values are displayed in conjunction with model calculations for different dislocation densities using the Debye–Callaway model (see the supplementary material). Calculations were performed for lattice thermal conductivity only as the electronic contribution to the total thermal conductivity is negligible for $SrTiO_3$ in the considered temperature range.[17] The measured magnitude of thermal conductivity of ~12 W $\mathrm{m}^{-1}\mathrm{K}^{-1}$ at room temperature is consistent with the literature,[16,17,21] and qualitative behavior agrees well with the calculated dependence.

Differences in thermal conductivity are within the error of measurements for single crystals and polycrystals, corroborated also for Fe- and Nb-doped crystals as well as ⟨110⟩{110} dislocation bands (see the supplementary material). The error of measurement, mostly stemming from the sample thickness [see the supplementary material

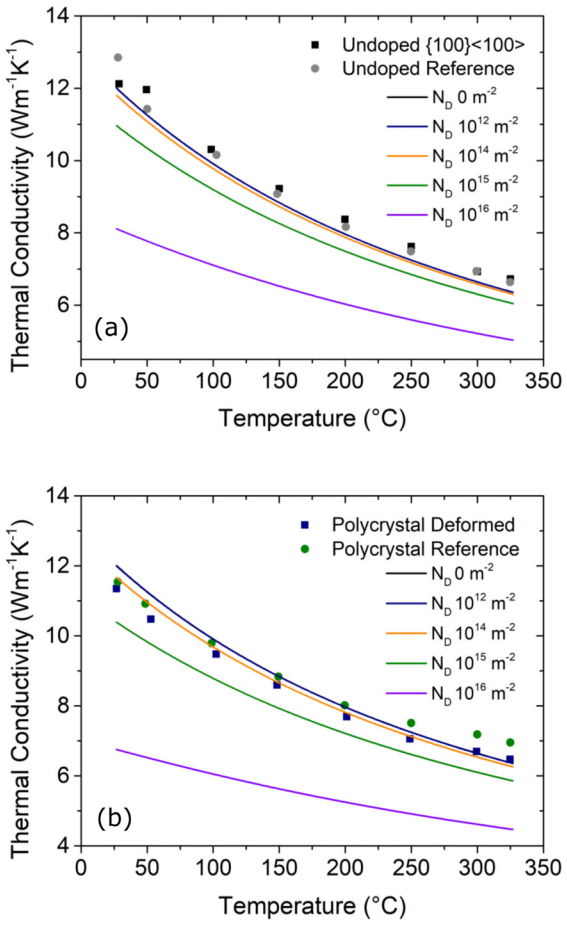

FIG. 3. Thermal conductivity of deformed single crystal (a) and polycrystal (b) compared to that of the corresponding reference sample along with calculated values for different dislocation densities. Curves for dislocation densities of 0 m^{-2} and $10^{12}\ \mathrm{m}^{-2}$ are coincident.

(Fig. S3)], was estimated to be 5% with a tendency to decrease with increasing temperature. The influence of the sample thickness on LFA results is a known phenomenon that could be corrected.[22] Nevertheless, samples of equal thickness were quantified in this study to ensure direct comparability with each other.

As the MFP in $SrTiO_3$ is only several nm according to our model calculations and literature,[23,24] intrinsic scattering lengths are short. Therefore, the mean dislocation distance of around 1 μm in deformed single crystals is not sufficient to achieve extrinsic scattering with a significant influence on the total MFP. According to the calculation, differences in thermal conductivity can be expected above a dislocation density of 10^{15} m^{-2}.

Dislocation density in the polycrystalline sample varies between different grains. The average dislocation density of 2×10^{12} m^{-2} is comparable to the single crystal and, hence, does not suffice to reduce thermal conductivity.

The reduction of thermal conductivity at room temperature due to phonon scattering by dislocations was reported for dislocations in grain boundaries[25] and above a critical dislocation density of 10^{11} m^{-2} in GaN.[11] Comparison of thermal properties of GaN and $SrTiO_3$ indicates that thermal conductivity of GaN with a value around 230 W m^{-1} K^{-1}[11] is much higher. Furthermore, phonons with a MFP greater than 1 μm have their main contribution to heat transfer at 309 K.[26] Hence, extrinsic scattering is expected to be achievable at lower dislocation densities in GaN than in $SrTiO_3$.

Simulations for thermoelectrics demonstrated that a significant reduction of thermal conductivity could be reached with dislocation densities of 10^{15} m^{-2} in PbTe.[27] Additionally, a significant reduction of thermal conductivity was obtained experimentally for dislocation densities of 10^{16} m^{-2} for PbTe.[6] The MFP of PbTe at 300 K is calculated to be around 1 nm.[28] Compared to $SrTiO_3$, the MFP of PbTe is shorter by a factor of around three.[23,24] Hence, the critical dislocation density for $SrTiO_3$ is expected to lie in-between the values for PbTe and GaN.

The approach of plastic deformation appears to be not a feasible tool for phonon engineering of thermoelectrics, which already have a low thermal conductivity due to high intrinsic scattering. Our model calculations predict a potential influence on thermal conductivity of $SrTiO_3$ for dislocation densities of 10^{15} m^{-2} and higher. Nevertheless, these higher dislocation densities on the order of 10^{15} m^{-2} may be achievable in oxides by severe plastic deformation using high pressure torsion.[29] However, note that a dislocation density of 3×10^{16} m^{-2} means that ⟨110⟩{110} type dislocations are only spaced 10 unit cells apart. They typically dissociate into two partials approximately four unit cells apart.[15,30] A higher density is, hence, not to be expected.

Ordered ⟨100⟩{100} dislocation networks with a dislocation density of 10^{12} m^{-2} in $SrTiO_3$ single crystals and of 2×10^{12} m^{-2} in $SrTiO_3$ polycrystals were obtained by plastic deformation. The resultant thermal conductivity between room temperature and 325 °C was comparable to that of undeformed reference samples. The results were affirmed for ⟨110⟩{110} dislocation bands as well as Fe- and Nb-doped $SrTiO_3$ [see the supplementary material (Fig. S3)] and calculations using the Debye–Callaway model. As phonons in $SrTiO_3$ and other thermoelectrics have a low intrinsic mean free path in the range of nanometers, alternative processing methods are required to reach higher dislocation densities of about 10^{15} m^{-2} to significantly suppress thermal conductivity.

See the supplementary material for images of etch pits, a description of the used Debye–Callaway model, and results of additional measurements.

AUTHORS' CONTRIBUTIONS

This research project was designed by Jürgen Rödel, Lukas Porz, and Jing-Feng Li. Melanie Johanning performed all the mechanical experiments with the assistance of Lukas Porz. Jinfeng Dong also contributed to the Debye–Callaway model calculations and participated in thermal conductivity measurements. Atsutomo Nakamura provided the TEM observations using ultra-high voltage electron microscopy. Melanie Johanning wrote the first version, and all the authors worked on modifying it.

Melanie Johanning, Lukas Porz, and Jürgen Rödel thank Wolfgang Rheinheimer for providing the polycrystalline $SrTiO_3$ and for critically reading this manuscript. They are also indebted to the Deutsche Forschungsgemeinschaft for funding this work under No. 414179371.

Atsutomo Nakamura acknowledges the financial support of JST PRESTO Grant Number JPMJPR199A and JSPS KAKENHI Grant Numbers JP19H05786 and JP18H03840, Japan. Ultra-high voltage electron microscopy (UHVEM) observations in this work were conducted in Nagoya Univ., supported by the Nanotechnology Platform Program of MEXT, Japan. We are grateful to Mr. K. Higuchi for technical assistance with UHVEM experiments.

J.-F. Li thanks the support of the basic science center project of NSFC under Grant No. 51788104.

DATA AVAILABILITY

The data that support the findings of this study are available within this article and its supplementary material.

REFERENCES

[1]Z. Liu, J. Mao, T.-H. Liu, and G. Chen, MRS Bull. **43**, 181 (2018).
[2]Z. Chen, X. Zhang, and Y. Pei, Adv. Mater. **30**, e1705617 (2018).
[3]D. Srivastava, C. Norman, F. Azough, M. C. Schäfer, E. Guilmeau, D. Kepaptsoglou, Q. M. Ramasse, G. Nicotra, and R. Freer, Phys. Chem. Chem. Phys. **18**, 26475 (2016); H. Muta, K. Kurosaki, and S. Yamanaka, J. Alloys Compd. **392**, 306 (2005); C.-C. Lin, R. Lydia, J. H. Yun, H. S. Lee, and J. S. Rhyee, Chem. Mater. **29**, 5344 (2017); Z.-G. Chen, G. Han, L. Yang, L. Cheng, and J. Zou, Prog. Nat. Sci.: Mater. Int. **22**, 535 (2012).
[4]S. I. Kim, K. H. Lee, H. A. Mun, H. S. Kim, S. W. Hwang, J. W. Roh, D. J. Yang, W. H. Shin, X. S. Li, Y. H. Lee, G. J. Snyder, and S. W. Kim, Science **348**, 109 (2015).
[5]Y. Pan, U. Aydemir, J. A. Grovogui, I. T. Witting, R. Hanus, Y. Xu, J. Wu, C.-F. Wu, F.-H. Sun, H.-L. Zhuang, J.-F. Dong, J.-F. Li, V. P. Dravid, and G. J. Snyder, Adv. Mater. **30**, e1802016 (2018).
[6]Z. Chen, Z. Jian, W. Li, Y. Chang, B. Ge, R. Hanus, J. Yang, Y. Chen, M. Huang, G. J. Snyder, and Y. Pei, Adv. Mater. **29**, 1606768 (2017).
[7]C. J. Vineis, A. Shakouri, A. Majumdar, and M. G. Kanatzidis, Adv. Mater. **22**, 3970 (2010).
[8]P. G. Klemens, Proc. Phys. Soc. A **68**, 1113 (1955).
[9]P. Carruthers, Phys. Rev. **114**, 995 (1959); A. Maurel, J.-F. Mercier, and F. Lund, Phys. Rev. B **70**, 24303 (2004); M. Li, Z. Ding, Q. Meng, J. Zhou, Y. Zhu, H. Liu, M. S. Dresselhaus, and G. Chen, Nano Lett. **17**, 1587 (2017).
[10]R. L. Sproull, M. Moss, and H. Weinstock, J. Appl. Phys. **30**, 334 (1959); M. Moss, *ibid.* **36**, 3308 (1965); A. Taylor, H. R. Albers, and R. O. Pohl, *ibid.* **36**, 2270 (1965).

[11]C. Mion, J. F. Muth, E. A. Preble, and D. Hanser, Appl. Phys. Lett. **89**, 092123 (2006).
[12]N. G. Error and U. Balachandran, J. Am. Ceram. Soc. **65**, 426 (1982).
[13]K. Szot, C. Rodenbücher, G. Bihlmayer, W. Speier, R. Ishikawa, N. Shibata, and Y. Ikuhara, Crystals **8**, 241 (2018).
[14]S. Taeri, D. Brunner, W. Sigle, and M. Rühle, Z. Metallkunde **95**, 433 (2004).
[15]L. Jin, X. Guo, and C. L. Jia, Ultramicroscopy **134**, 77 (2013).
[16]T. Tadano and S. Tsuneyuki, Phys. Rev. B **92**, 054301 (2015).
[17]V. Martelli, J. L. Jiménez, M. Continentino, E. Baggio-Saitovitch, and K. Behnia, Phys. Rev. Lett. **120**, 125901 (2018).
[18]H. Ohta, Mater. Today **10**, 44 (2007); J. W. Fergus, J. Eur. Ceram. Soc. **32**, 525 (2012); M. Ohtaki, J. Ceram. Soc. Jpn. **119**, 770 (2011).
[19]Y. Yin, B. Tudu, and A. Tiwari, Vacuum **146**, 356 (2017).
[20]H. Ohta, K. Sugiura, and K. Koumoto, Inorg. Chem. **47**, 8429 (2008).
[21]S. Ohta, T. Nomura, H. Ohta, and K. Koumoto, J. Appl. Phys. **97**, 34106 (2005); L. Zhang, N. Li, H.-Q. Wang, Y. Zhang, F. Ren, X.-X. Liao, Y.-P. Li, X.-D. Wang, Z. Huang, Y. Dai, H. Yan, and J.-C. Zheng, Chin. Phys. B **26**, 16602 (2017).
[22]P. Schoderböck, H. Klocker, L. S. Sigl, and G. Seeber, Int. J. Thermophys. **30**, 599 (2009); G. V. Kuznetov and M. D. Kats, Meas. Tech. **55**, 454 (2012).
[23]N. Wang, H. Li, Y. Ba, Y. Wang, C. Wan, K. Fujinami, and K. Koumoto, J. Electron. Mater. **39**, 1777 (2010).
[24]S. Bhattacharya, A. Mehdizadeh Dehkordi, S. Tennakoon, R. Adebisi, J. R. Gladden, T. Darroudi, H. N. Alshareef, and T. M. Tritt, J. Appl. Phys. **115**, 223712 (2014).
[25]X. Meng, Z. Liu, B. Cui, D. Qin, H. Geng, W. Cai, L. Fu, J. He, Z. Ren, and J. Sui, Adv. Energy Mater. **7**, 1602582 (2017); H.-S. Kim, S. D. Kang, Y. Tang, R. Hanus, and G. Jeffrey Snyder, Mater. Horiz. **3**, 234 (2016).
[26]J. P. Freedman, J. H. Leach, E. A. Preble, Z. Sitar, R. F. Davis, and J. A. Malen, Sci. Rep. **3**, 2963 (2013).
[27]Y. Sun, Y. Zhou, J. Han, W. Liu, C. Nan, Y. Lin, M. Hu, and B. Xu, npj Comput. Mater. **5**, 97 (2019).
[28]B. Qiu, H. Bao, G. Zhang, Y. Wu, and X. Ruan, Comput. Mater. Sci. **53**, 278 (2012).
[29]K. Edalati, Adv. Eng. Mater. **21**, 1800272 (2019).
[30]P. Hirel, M. Mrovec, and C. Elsässer, Acta Mater. **60**, 329 (2012).